Contribution from the Division of Chemical and Physical Sciences, Deakin University, Waurn Ponds 3217, Australia, and Department of Inorganic Chemistry, University of Melbourne, Parkville 3052, Australia

Examination of Mercury Dithiocarbamate–Trialkylphosphine Mixed-Ligand Complexes by Electrochemical Techniques at Mercury Electrodes and Multinuclear Magnetic Resonance Spectroscopy

Alan M. Bond,*[1] Ray Colton,[2] Anthony F. Hollenkamp,[1] and John E. Moir[1]

Received May 6, 1985

Electrochemical studies at mercury electrodes of mercury(II) dithiocarbamates, $Hg(RR'dtc)_2$, and mercury(II) trialkylphosphine complexes, $[Hg(PX_3)_2]^{2+}$, or their respective ligands, in dichloromethane produce well-defined diffusion-controlled reduction or oxidation processes. Remarkably, the electrochemistry of the mixtures $Hg(RR'dtc)_2$ and PX_3, $[Hg(PX_3)_2]^{2+}$ and $RR'dtc^-$, and $Hg(RR'dtc)_2$ and $[Hg(PX_3)_2]^{2+}$ gives rise to current reversal (cyclic voltammetry), negative differential current (differential pulse polarography), and current suppression (dc polarography) as well as new reduction processes. Previously such phenomena have been associated with surface or electrostatic effects or with catalytic electrochemical processes and not with mixed-ligand formation as appears to be the present case. Multinuclear magnetic resonance studies (^{199}Hg and ^{31}P) have been used to study the nature of these mixed-ligand complexes, and thermodynamic parameters of the reaction $Hg(RR'dtc)_2PX_3 + PX_3 \rightleftarrows Hg(RR'dtc)_2(PX_3)_2$ have been calculated. An explanation for the unusual electrochemical phenomena based on mixed-ligand-complex formation is arrived at from the combined use of electrochemical and NMR data.

Introduction

Mixed-ligand complexes of the type MX_aY_b are of considerable interest in many fields of chemistry, and with particular relevance to this work, the relationship of the mixed-ligand complexes to the individual compounds MX_n and MY_m has been studied extensively.[3]

Nuclear magnetic resonance (NMR) spectroscopy has been widely used to study the type of reaction

$$MX_n + MY_m \underset{k_b}{\overset{k_f}{\rightleftharpoons}} 2MX_{n/2}Y_{m/2} \qquad (1)$$

Distinctly different spectra may be observed, depending on thermodynamic and kinetic considerations (values of k_f and k_b).[4,5] If exchange is rapid on the NMR time scale, then an average NMR signal is observed for the different species while for slow exchange individual signals for each of the compounds MX_n, MY_m, and $MX_{n/2}Y_{m/2}$ may be observed. Intermediate rates of exchange produce more complex spectra from which kinetic data may be calculated.[6,7]

In the area of electrochemistry, studies on mixed-ligand complexes have also been reported. When all participating species are in rapid exchange (diffusion-controlled), a single voltammetric response is observed. This situation has been treated theoretically and experimentally by Schaap and McMasters[8] for the case where reduction to the metal occurs. In contrast, oxidation of mixtures of FeL_3 and FeL'_3 (L = c-Hx_2dtc, L' = Bz_2dtc (see Appendix for definition of symbols)) under the conditions of alternating-current voltammetry produces four peaks that can be assigned to the redox processes[9]

$$FeL_nL'_{3-n} \rightleftarrows [FeL_nL'_{3-n}]^+ + e^- \qquad n = 0\text{–}3 \qquad (2)$$

even though the iron dithiocarbamate system is known to be labile on the synthetic time scale. This situation closely parallels the case of slow exchange in NMR.

In our laboratories, the electrochemical reduction processes for $Hg(RR'dtc)_2$[10] and $[Hg(PX_3)_2](ClO_4)_2$[11] have been investigated in dichloromethane solution. NMR studies in the same solvent demonstrate[12] that mixed-ligand complexes are formed by the reaction

$$Hg(RR'dtc)_2 + nPX_3 \rightleftarrows Hg(RR'dtc)_2(PX_3)_n \qquad X = n\text{-Bu, } c\text{-Hx};\ n = 1, 2 \qquad (3)$$

By observation of both ^{199}Hg and ^{31}P NMR spectra, this system was shown to undergo rapid exchange at room temperature, but at very low temperatures (approximately −100 °C) signals for individual species may be observed.

As part of our continuing studies employing the combination of multinuclear magnetic resonance and electrochemical techniques,[13–15] it was thought appropriate to investigate the electrochemical consequences of mixed-ligand-complex formation in systems where the time domain for exchange is known from NMR studies to be less than diffusion-controlled. Remarkably, electrochemical studies produced totally unexpected data that are entirely different from the data describing the electrochemical behavior of the individual complexes $Hg(RR'dtc)_2$[10] and $[Hg(PX_3)_2](ClO_4)_2$.[11] In this paper we report these unexpected electrochemical results and present an interpretation based on the combined use of NMR and electrochemical techniques.

Experimental Section

Materials. All solvents were of HPLC or analytical reagent grade. The tetrabutylammonium perchlorate used as the supporting electrolyte was of electrochemical grade, and all other chemicals used were of analytical reagent grade.

Preparations. (a) $Hg(RR'dtc)_2$. These complexes were prepared by a modification of a method described in the literature.[16] A solution of the sodium dithiocarbamate was prepared by addition of CS_2 to a chilled aqueous mixture of sodium hydroxide and the appropriate secondary amine, all in stoichiometric quantities. To this solution was added the stoichiometric amount of mercury(II) nitrate. The resulting precipitate was then filtered off, dried, and purified by Soxhlet extraction into chloroform.

(1) Deakin University.
(2) University of Melbourne.
(3) Colton, R.; Dakternieks, D.; Harvey, C.-A. *Inorg. Chim. Acta* **1982**, *61*, 1.
(4) Colton, R.; Dakternieks, D. *Inorg. Chim. Acta* **1983**, *71*, 101.
(5) Colton, R.; Dakternieks, D. *Aust. J. Chem.* **1980**, *33*, 2405.
(6) Anker, M. W.; Colton, R.; Rix, C. J. *Aust. J. Chem.* **1971**, *24*, 1157.
(7) *Dynamic Nuclear Magnetic Resonance Spectroscopy*; Jackman, L. M., Cotton, F. A., Eds.; Academic: New York, 1975.
(8) Schaap, W. B.; McMasters, D. L. *J. Am. Chem. Soc.* **1961**, *83*, 4699.
(9) Chant, R.; Hendrickson, A. R.; Martin, R. L.; Rohde, N. M. *Inorg. Chem.* **1975**, *14*, 1894.
(10) Bond, A. M.; Colton, R.; Dillon, M. L.; Moir, J. E.; Page, D. R. *Inorg. Chem.* **1984**, *23*, 2883.
(11) Bond, A. M.; Colton, R.; Dakternieks, D.; Hanck, K. W.; Svestka, M. *Inorg. Chem.* **1983**, *22*, 236.
(12) Bond, A. M.; Colton, R.; Dakternieks, D.; Dillon, M. L.; Hauenstein, J.; Moir, J. E. *Aust. J. Chem.* **1981**, *34*, 1393.
(13) Bond, A. M.; Colton, R.; Dakternieks, D.; Hanck, K. W. *Inorg. Chem.* **1982**, *21*, 117.
(14) Bond, A. M.; Carr, S. W.; Colton, R.; Kelly, D. P. *Inorg. Chem.* **1983**, *22*, 989.
(15) Bond, A. M.; Colton, R.; Dillon, M. L.; Hollenkamp, A. F.; Moir, J. E. *Inorg. Chem.* **1985**, *24*, 1591.
(16) Coucouvanis, D. *Prog. Inorg. Chem.* **1970**, *11*, 276.

0020-1669/86/1325-1519$01.50/0

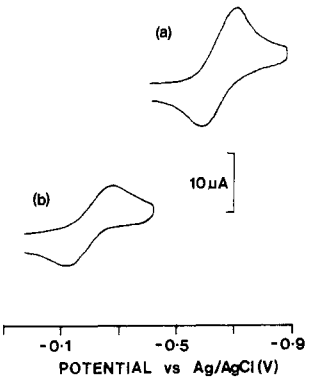

Figure 1. Cyclic voltammograms at a HMDE for the reduction of 5×10^{-4} M (a) $Hg(n\text{-}Bu_2dtc)_2$ and (b) $[Hg(P\text{-}c\text{-}Hx_3)_2](ClO_4)_2$ in CH_2Cl_2 (0.1 M Bu_4NClO_4, 20 °C, scan rate 500 mV s^{-1}).

(b) $Bu_4N(RR'dtc)$. The use of tetrabutylammonium hydroxide (40% w/w in water) in place of sodium hydroxide in (a) yielded a pale yellow solid of tetrabutylammonium dithiocarbamate, which was recrystallized from ethanol.

(c) $[Hg(PX_3)_2](ClO_4)_2$. Following the method of Alyea et al.,[17] we prepared these complexes by stirring a stoichiometric mixture of mercury(II) perchlorate with the appropriate phosphine ligand in ethanol. All products were white solids and were recrystallized from dichloromethane/ether.

Instrumental Methods. (a) Electrochemistry. Voltammetric measurements were made with a Princeton Applied Research Corp. (Princeton, NJ) Model 174A polarographic analyzer. Either a dropping-mercury electrode (dc and differential pulse polarography) or a hanging-mercury-drop electrode (cyclic voltammetry) was used as the working electrode with a platinum-wire auxiliary electrode and a Ag/AgCl (saturated LiCl; CH_2Cl_2) reference electrode. The $[(C_5H_5)_2Fe]^+/(C_5H_5)_2Fe$ redox couple was also measured frequently (oxidation of 5×10^{-4} M ferrocene) to provide an internal check on the stability of the reference electrode. In the case where a solid-mercury electrode was required for low-temperature studies, the following procedure was used: A small gold-disk electrode was first cleaned and then polished with fine alumina. Immersion of the clean surface in mercury left a mercury film on the electrode, which solidified when the temperature of the solution being investigated was taken below −39 °C. Unless otherwise specified, all measurements were made at 20 °C in dichloromethane containing 0.1 M Bu_4NClO_4 and the concentration of the $Hg(RR'dtc)_2$ and $[Hg(PX_3)_2]^{2+}$ compounds used was 5×10^{-4} M.

Controlled-potential-electrolysis experiments were performed at a mercury-pool electrode with a PAR Model 173 pontentiostat/galvanostat in conjunction with a Model 179 digital coulometer. The platinum-gauze auxiliary electrode was isolated from the test solution via a salt bridge, and the reference electrode was identical with that used for polarographic measurements.

(b) NMR Spectroscopy. The mercury-199 and phosphorus-31 NMR spectra of dichloromethane solutions were recorded with broad-band proton decoupling on a JEOL FX 100 spectrometer using an external ^7Li lock. ^{199}Hg spectra were recorded at 17.76 MHz with a 20-kHz spectral window (acquisition time 0.2 s, 8192 data points), while phosphorus spectra were recorded under similar conditions at 40.26 MHz. Chemical shifts were referenced against 1 M phenylmercury acetate in Me_2SO and 85% aqueous phosphoric acid with use of the high frequency positive convention. Spectra were recorded in the presence of $Cr(acac)_3$ to reduce the relaxation time for ^{199}Hg nuclei and also to ensure that integration of phosphorus peaks gave a true measure of the concentration of various species. A JEOL NM 5471 controller was used to control the probe temperature and calibrated against a platinum resistance thermometer.

(c) Molecular Weight Measurements. Molecular weights in dichloromethane solution were determined with a Hitachi Perkin-Elmer Model 115 molecular weight apparatus. A linear response was obtained for concentrations of the calibrant (benzil) over the range 1×10^{-4} to 1×10^{-2} M.

Results and Discussion

Figure 1 shows cyclic voltammograms at a HMDE for the reduction processes of $Hg(n\text{-}Bu_2dtc)_2$ and $[Hg(P\text{-}c\text{-}Hx_3)_2](ClO_4)_2$ in dichloromethane at 20 °C. The ligands, $n\text{-}Bu_2dtc^-$ and P-c-Hx_3, give chemically reversible oxidation responses at the same potentials as the mercury complexes.[10,11] The overall processes can therefore be written as

$$Hg(RR'dtc)_2 + 2e^- \rightleftarrows Hg + 2RR'dtc^- \quad (4)$$

$$[Hg(PX_3)_2]^{2+} + 2e^- \rightleftarrows Hg + 2PX_3 \quad (5)$$

In both cases a mercury(I) intermediate is presumed to participate in the redox process so that eq 4 and 5 may be rewritten as

$$\begin{aligned} Hg(RR'dtc)_2 + Hg &\rightleftarrows 2HgRR'dtc \\ 2HgRR'dtc + 2e^- &\rightleftarrows 2Hg + 2RR'dtc^- \end{aligned} \quad (6)$$

$$\begin{aligned} [Hg(PX_3)_2]^{2+} + Hg &\rightleftarrows 2[Hg(PX_3)]^+ \\ 2[Hg(PX_3)]^+ + 2e^- &\rightleftarrows 2Hg + 2PX_3 \end{aligned} \quad (7)$$

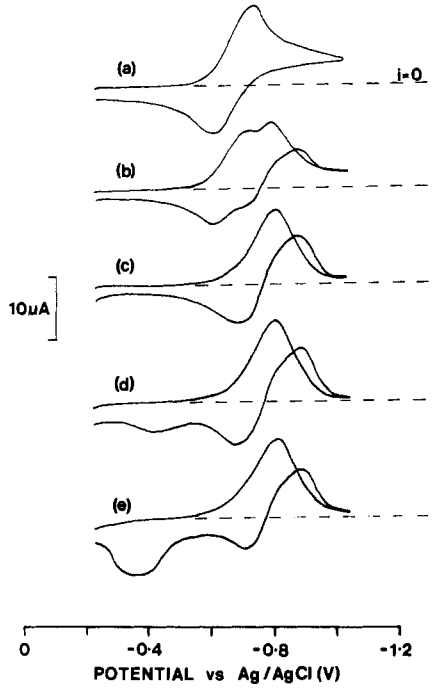

Figure 2. Cyclic voltammograms for a solution of $Hg(n\text{-}Bu_2dtc)_2$ (5×10^{-4} M) after addition of (a) 0, (b) 2.5×10^{-4}, (c) 5×10^{-4}, (d) 1×10^{-3}, and (e) 1.5×10^{-3} M P-c-Hx_3. Experimental conditions are the same as for Figure 1.

Addition of tricyclohexylphosphine, P-c-Hx_3, to a solution of $Hg(n\text{-}Bu_2dtc)_2$ produces the result shown in Figure 2. Since the half-wave potential for the $[Hg(P\text{-}c\text{-}Hx_3)_2]^{2+}/P\text{-}c\text{-}Hx_3$ couple is approximately 0.4 V more positive than that for the $Hg(n\text{-}Bu_2dtc)_2/n\text{-}Bu_2dtc^-$ couple, one might expect to see a positive shift in the potential of the reversible process. In fact, a new process arises with a concomitant decrease in the magnitude of the wave for the $Hg(n\text{-}Bu_2dtc)_2$ reduction process. This new process, which appears approximately 100 mV more negative than the dithiocarbamate reduction, is characterized by a current crossover on the positive-direction scan. The process attributable to the P-c-Hx_3 ligand is greatly suppressed and modified until the ratio of $Hg(n\text{-}Bu_2dtc)_2$ to P-c-Hx_3 reaches 1:2. When this ratio is exceeded, the current for the process

$$2P\text{-}c\text{-}Hx_3 + Hg \rightleftarrows [Hg(c\text{-}Hx_3)_2]^{2+} + 2e^- \quad (8)$$

increases in proportion to further additions of ligand.

Addition of tetrabutylammonium di-*n*-butyldithiocarbamate, $Bu_4N[n\text{-}Bu_2dtc]$, to a solution of $[Hg(P\text{-}c\text{-}Hx_3)_2](ClO_4)_2$ (Figure 3) leads to complete removal of the reduction response for the latter. At the stage when the ratio of the phosphine complex to dithiocarbamate is 1:1, the appearance of a new wave at more negative potentials is noted with current reversal apparent. A small wave at about −0.4 V is also observed. Complexes of the kind $[Hg(P\text{-}c\text{-}Hx_3)_2(RR'dtc)]^+$ are indicated. When the ratio of mercury complex to dithiocarbamate ligand is 1:2 (Figure 3c), the response is identical with that in Figure 2, where Hg(*n*-

(17) Alyea, E. C.; Dias, S. A.; Goel, R. G.; Ogini, W. G.; Pilon, P.; Meek, D. W. *Inorg. Chem.* **1978**, *17*, 1697.

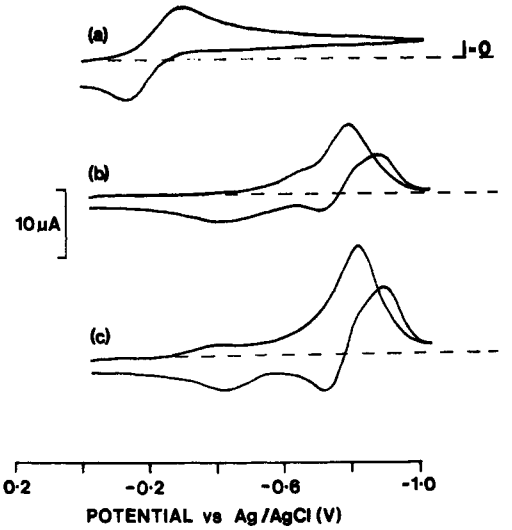

Figure 3. Cyclic voltammograms for a solution of $[Hg(P\text{-}c\text{-}Hx_3)_2](ClO_4)_2$ (5×10^{-4} M) after addition of (a) 0, (b) 5×10^{-4}, and (c) 1×10^{-3} M $Bu_4N(n\text{-}Bu_2dtc)$. Experimental conditions are the same as for Figure 1.

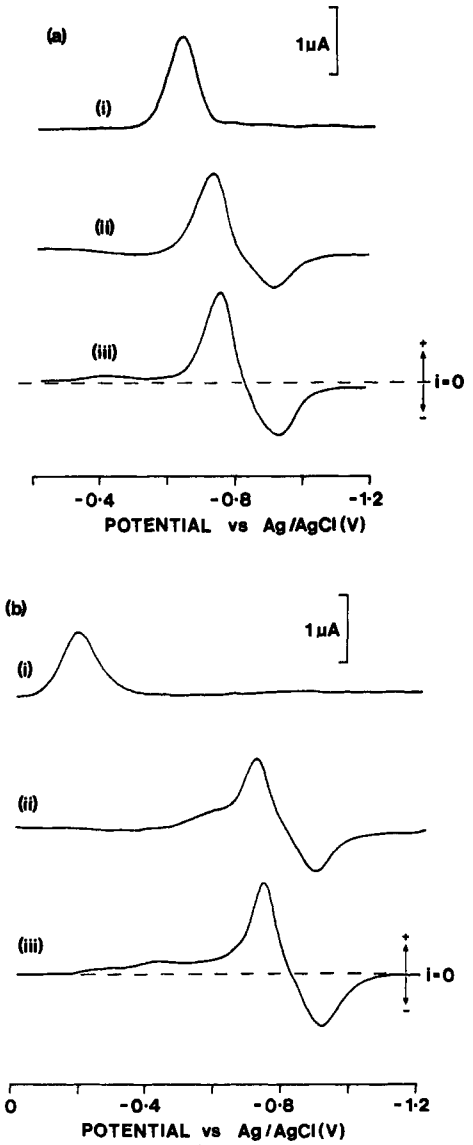

Figure 4. Differential pulse polarograms for (a) a solution of $Hg(n\text{-}Bu_2dtc)_2$ (5×10^{-4} M) with P-c-Hx_3 present at (i) 0, (ii) 5×10^{-4}, and (iii) 1×10^{-3} M and (b) a solution of $[Hg(P\text{-}c\text{-}Hx_3)_2](ClO_4)_2$ (5×10^{-4} M) with $Bu_4N(n\text{-}Bu_2dtc)$ present at (i) 0, (ii) 5×10^{-4}, and (iii) 1×10^{-3} M (drop time 0.5 s, pulse amplitude −50 mV).

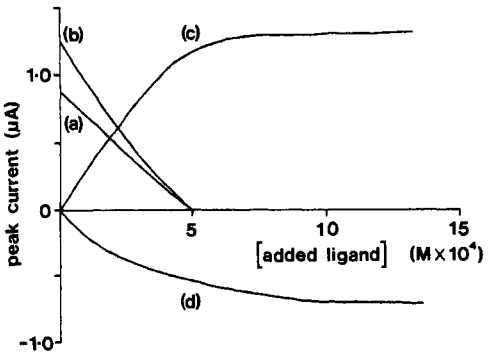

Figure 5. Plots of peak height (i_p; differential pulse polarography) vs. concentration of free ligand added to a 5×10^{-4} M solution of a mercury complex. The responses were observed for (a) $[Hg(P\text{-}c\text{-}Hx_3)_2](ClO_4)_2$ (E_p = −0.21 V), addition of $Bu_4N(n\text{-}Bu_2dtc)$, (b) $Hg(n\text{-}Bu_2dtc)_2$ (E_p = −0.66 V), addition of P-c-Hx_3, (c) $Hg(n\text{-}Bu_2dtc)_2$(P-c-Hx_3) (E_p = −0.74 V), addition of P-c-Hx_3 to $Hg(n\text{-}Bu_2dtc)_2$, and (d) the process giving the negative differential current (E_p = −0.92 V), addition of P-c-Hx_3 to $Hg(n\text{-}Bu_2dtc)_2$.

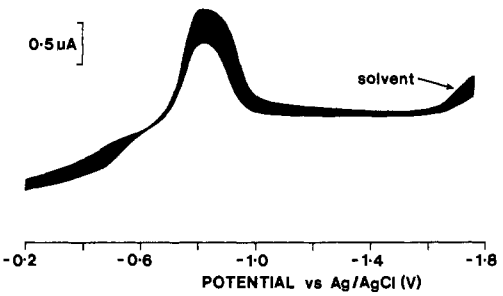

Figure 6. Dc polarogram (drop time 0.5 s) for the reduction response of a solution containing $Hg(n\text{-}Bu_2dtc)_2$ (5×10^{-4} M) and P-c-Hx_3 (1×10^{-3} M).

$Bu_2dtc)_2$:P-c-Hx_3 is 1:2. At ratios in excess of 1:2 $[Hg(P\text{-}c\text{-}Hx_3)_2]^{2+}$:$n$-$Bu_2dtc^-$, the dithiocarbamate that is free in solution breaks down rapidly, giving rise to a series of oxidation waves.

Differential pulse polarograms provide higher resolution data for studying the phenomena attributable to mixed-ligand complexes. Figure 4 shows the results of differential pulse experiments that were equivalent to those utilizing cyclic voltammetry. The current reversal at a stationary mercury electrode under the conditions of cyclic voltammetry is observed as a negative differential current.

Whenever mixtures of $Hg(n\text{-}Bu_2dtc)_2$ and P-c-Hx_3 or $[Hg(P\text{-}c\text{-}Hx_3)_2]^{2+}$ and n-Bu_2dtc^- are present, the negative differential peak is observed always reaching a maximum when the ratio of the mercury complex to the ligand reaches 1:2. In both cases, when the ratio exceeds 1:2, responses for the free ligand (phosphine or dithiocarbamate) are observed as oxidation processes. All electrochemical data are summarized in Table I.

Figure 5 shows a series of what are effectively titration curves for the different responses including the negative differential peak from differential pulse polarography. Many of the electrode processes shown have close to stoichiometric relationships between the mercury complex:ligand ratio and the current associated with each process.

Neither cyclic voltammetry nor differential pulse polarography readily defines the sign of the current associated with different electrode processes. In contrast, dc polarography is an excellent source of this important information. Figure 6 shows that the current reversal (cyclic voltammetry) and negative differential current (differential pulse polarography) are related to a sharp depression of current in the limiting-current region. The limiting current, for a solution in which the ratio of mercury complex to ligand is 1:2, approaches background current at potentials more negative than −1.4 V (see Table I). However, the current never becomes less than background and is a function of potential. Figure 7 demonstrates that the magnitude of the suppression of limiting current is proportional to the concentration ratio Hg(*n*-

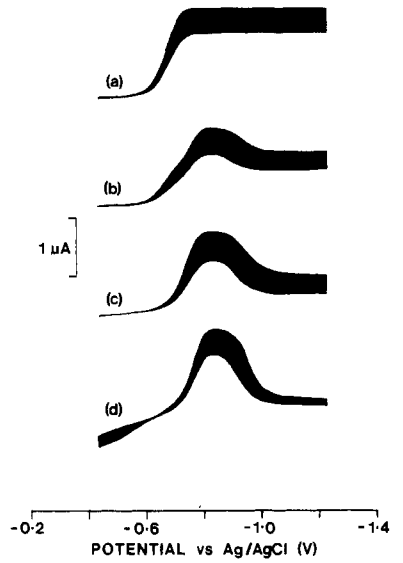

Figure 7. Dc polarograms (drop time 0.5 s) for a solution of $Hg(n\text{-}Bu_2dtc)_2$ (5×10^{-4} M) with P-c-Hx_3 present at (a) 0, (b) 2.5×10^{-4}, (c) 5×10^{-4}, and (d) 1×10^{-3} M.

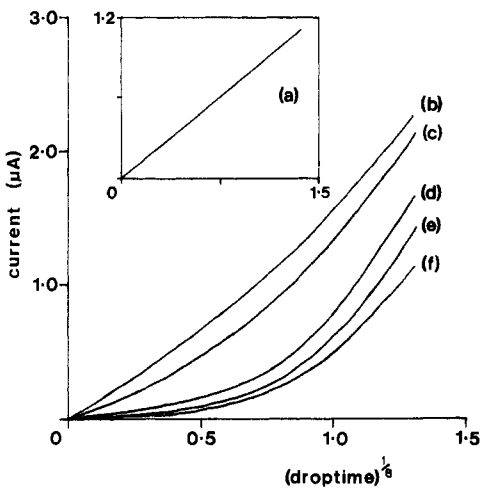

Figure 8. Dependence of current (dc polarography) on $t^{1/6}$ (as a function of potential for a solution containing $Hg(n\text{-}Bu_2dtc)_2$ (5×10^{-4} M) and P-c-Hx_3 (5×10^{-4} M): (a) −0.73 V; (b) −0.8 V; (c) −0.9 V; (d) −1.0 V; (e) −1.2 V; (f) −1.4 V.

$Bu_2dtc)_2$:P-c-Hx_3. Importantly, the limiting current prior to the onset of current suppression remains at the known value for the diffusion-controlled two-electron-reduction process of $Hg(n\text{-}Bu_2dtc)_2$.

When the ratio of $Hg(n\text{-}Bu_2dtc)_2$ to P-c-Hx_3 is 1:1, the new wave ($E_{1/2}$ = −0.73 V) is fully developed (current due to the reduction process for $Hg(n\text{-}Bu_2dtc)_2$ is zero) but the minimum current at negative potentials has not decreased to the background level. In this situation, time dependence studies of the current can be carried out with reasonable precision. Data are summarized in Figure 8. At $E_{1/2}$, the linear relationship between current and $t^{1/6}$ expected[18] for a diffusion-controlled process is closely approximated. At more negative potentials departure from diffusion control is apparent. In fact, limiting currents appear to be kinetically controlled, the current suppression being greater as the potential becomes more negative.

Further evidence of the kinetic nature of the currents for the mixed-ligand system was obtained from temperature dependence studies as shown in Figure 9. Comparison with equivalent figures (Figures 6, 4, and 2d, respectively) shows the depression in dc polarographic limiting current to be less at low temperatures, as

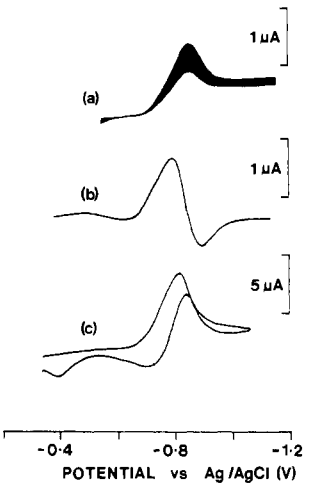

Figure 9. Responses for a solution containing $Hg(n\text{-}Bu_2dtc)_2$ (5×10^{-4} M) and P-c-Hx_3 (1×10^{-3} M): (a) dc polarogram (drop time 0.5 s, −39 °C); (b) differential pulse polarogram (drop time 0.5 s, pulse amplitude −50 mV, −39 °C); (c) cyclic voltammogram (solid-mercury electrode, scan rate 500 mV s^{-1}, −70 °C).

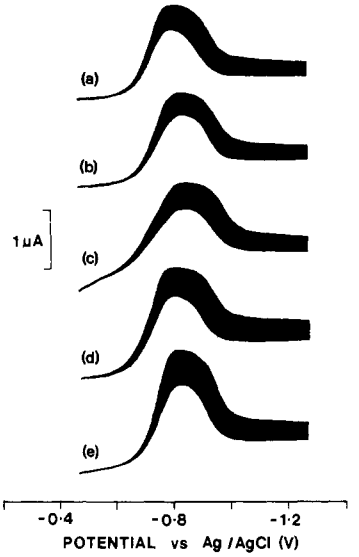

Figure 10. Dc polarograms (drop time 0.5 s) for solutions containing $Hg(n\text{-}Bu_2dtc)_2$ (5×10^{-4} M) and P-c-Hx_3 (5×10^{-4} M) with (a) 0.1 M Bu_4NClO_4, (b) 0.05 M Et_4NClO_4, (c) 0.1 M Hx_4NClO_4, (d) 0.1 M Bu_4NPF_6, and (e) 0.1 M Bu_4NBPh_4 as supporting electrolyte.

is also the case with negative differential peak currents. Interestingly, even at −70 °C, cyclic voltammograms on a solid-mercury electrode still show very clear evidence of current reversal. In fact, under any conditions of temperature and time domain available, it was found impossible to eliminate the unexpected responses observed in the presence of mixed-ligand-complex formation.

Many complex electrochemical mechanisms exhibit pronounced concentration dependence. Table II summarizes the data from differential pulse polarograms for solutions containing $Hg(n\text{-}Bu_2dtc)_2$ and P-c-Hx_3 in a 1:2 mole ratio over the concentration range 5×10^{-4} to 1×10^{-5} M. Within experimental error the ratio of the currents for the reduction process and the negative differential peak is independent of concentration over this range. The position of the minimum is essentially independent of concentration. Current reversal behavior was also apparent over the range of solution concentrations.

Many phenomena associated with minima in dc polarography have been attributed to double-layer effects.[19-23] When unusual

(18) Meites, L. *Polarographic Techniques*, 2nd ed.; Interscience: New York, 1965; p 95.

(19) Nagaosa, Y.; Tanaka, I. *Bull. Chem. Soc. Jpn.* **1984**, *57*, 589.
(20) Fawcett, W. R.; Mackey, M. D. *J. Electroanal. Chem. Interfacial Electrochem.* **1970**, *27*, 219.

Table I. Voltammetric Data for the Reduction Processes of Mixed-Ligand Complexes $Hg(n\text{-}Bu_2dtc)_2(P\text{-}c\text{-}Hx_3)_n$ (n = 1, 2) at Mercury Electrodes in Dichloromethane (0.1 M Bu_4NClO_4) at 20 °C

			dc polarography[a]			differential pulse polarography[b]				cyclic voltammetry[c]					
$[HgL_2]$,[d] M	$[HgL'_2]^{2+}$,[e] M	[L],[d] M	[L'],[e] M	$E_{1/2}$, V[f]	i_l,[f] μA	i_l,[g] μA	E_p, V[f]	i_p, μA	E_p,[h] V[f]	i_p,[h] μA	E_p^{red}, V[f]	i_p^{red}, μA	E_p^{ox}, V[f]	i_p^{ox}, μA	$E_p^{cr\,i}$, V[f]	$i_p^{cr\,i}$, μA
5×10^{-4}	0	0	0	−0.660	1.39	1.39	−0.665	1.25			−0.730	13.0	−0.605	−11.4		
5×10^{-4}	0	0	5×10^{-4}	−0.725	1.32	0.05	−0.740	1.18	−0.920	−0.48	−0.805	12.8	−0.685	−12.2	−0.890	8.3
5×10^{-4}	0	0	1×10^{-3}	−0.740	1.43	0.12	−0.750	1.30	−0.920	−0.70	−0.810	13.2	−0.710	−12.2	−0.895	8.9
0	5×10^{-4}	0	0	−0.205	1.22	1.26	−0.205	0.88			−0.300	7.1	−0.140	−6.7		
0	5×10^{-4}	5×10^{-4}	0	−0.730	1.26	0.45	−0.735	0.97	−0.915	−0.52	−0.790	7.9	−0.705	−5.9	−0.880	5.5
0	5×10^{-4}	1×10^{-3}	0	−0.745	1.41	0.15	−0.755	1.30	−0.925	−0.67	−0.810	13.4	−0.710	−11.0	−0.890	7.9

[a] Dropping-mercury electrode, t = 0.5 s. [b] Pulse amplitude −50 mV. [c] Hanging-mercury-drop electrode, v = 500 mV s^{-1}. [d] L = $[n\text{-}Bu_2dtc]^-$. [e] L' = P-c-Hx_3. [f] Measured at E = −0.8 V. [g] Measured at E = −1.4 V. [h] Peak corresponding to negative differential current i_p. [i] Peak of current reversal. [j] V vs. Ag/AgCl (satd LiCl; CH_2Cl_2). $E_{1/2}[(C_5H_5)_2Fe^+/(C_5H_5)_2Fe]$ = +0.480 V vs. Ag/AgCl (satd LiCl; CH_2Cl_2).

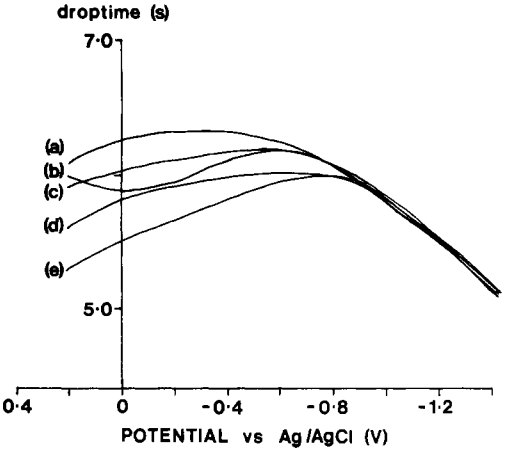

Figure 11. Electrocapillary curves for (a) 0.1 M Bu_4NClO_4 in CH_2Cl_2, with additions of (b) $[Hg(P\text{-}c\text{-}Hx_3)_2](ClO_4)_2$ (5×10^{-4} M), (c) P-c-Hx_3 (5×10^{-4} M), (d) $Hg(n\text{-}Bu_2dtc)_2$ (5×10^{-4} M) and P-c-Hx_3 (5×10^{-4} M), and (e) $Hg(n\text{-}Bu_2dtc)_2$ (5×10^{-4} M).

current–potential effects arise in this way, a substantial dependence of the responses on the nature of the supporting electrolyte is noted. Figure 10 shows that while some dependence on the supporting electrolyte is observed, significant changes in the nature of the cation or anion of the supporting electrolyte produce only minor changes in the pattern of behavior. This data suggests that the interaction of any charged species with the double layer is not the dominant phenomenon contributing to the observed responses.

Surface phenomena can also lead to severely distorted electrochemical responses.[24] Figure 11 shows electrocapillary curves for a series of compounds that participate in mixed-ligand-complex formation, as well as for the solvent (0.1 M Bu_4NClO_4) in dichloromethane. At negative potentials, where dc polarographic currents are severely depressed, there is no evidence for strong adsorption. At more positive potentials differing degress of adsorption are indicated.

Controlled-potential electrolysis experiments were carried out at a mercury-pool electrode for solutions containing $Hg(n\text{-}Bu_2dtc)_2$ and P-c-Hx_3 in the mole ratios 1:1 and 1:2. With the potential fixed at −0.80 V (region of maximum current) the electrolysis proceeds rapidly to produce free dithiocarbamate and free phosphine ligands (electrochemical identification) via a two-electron reduction. Shifting the potential to −1.4 V (region of greatest current suppression) results in an extremely slow electrolysis (3–4 h). As expected, initial currents are similar regardless of the potential but after a short time the electrolysis slows due to the processes in solution that cause current suppression. Product characterization after this slow controlled-potential electrolysis is complicated by the decomposition of the dithiocarbamate ion in dichloromethane solution.

A series of experiments with $Hg(RR'dtc)_2$ (R = R' = c-Hx and RR' = pyrr) and additions of P-c-Hx_3 to give 1:1 and 1:2 mole ratios of mercury dithiocarbamate to phosphine showed behavior qualitatively similar to that described above for R = R' = n-Bu. In a similar fashion, experiments with mixtures of $Hg(n\text{-}Bu_2dtc)_2$ and PX_3 showed behavior similar to that for P-c-Hx_3 when X = Bu; however when X = Ph, no changes to the reduction response of $Hg(n\text{-}Bu_2dtc)_2$ were observed. Current reversal and negative differential peaks were absent, and the oxidation response for free PPh_3 was observed to accurately reflect the amount of phosphine added to the solution. Table III summarizes polarographic data for the different combinations of complexes and ligands studied. From these results it appears that the basicity of the phosphine

(21) Fawcett, W. R.; Bieman, D. J.; Mackey, M. D. *Collect. Czech. Chem. Commun.* **1971**, *36*, 503.
(22) Fawcett, W. R.; Kuo Lee, Y. C. *Can. J. Chem.* **1971**, *49*, 2657.
(23) Pospíšil, L.; DeLevie, R. *J. Electroanal. Chem. Interfacial Electrochem.* **1970**, *25*, 245.
(24) Müller, E.; Emons, H.; Dörfler, H.-D.; Lipkowski, J. *J. Electroanal. Chem. Interfacial Electrochem.* **1982**, *142*, 39.

Table II. Concentration Dependence of Differential Pulse Polarograms[a] for a $Hg(RR'dtc)_2$:P-c-Hx_3 Mole Ratio of 1:2 in Dichloromethane (0.1 M Bu_4NClO_4) at 20 °C

$[Hg(n\text{-}Bu_2dtc)_2]$, M	E_p, V[c]	i_p, μA	E_p^*,[b] V[c]	i_p^*, μA	$-i_p^*/i_p$	$E_p - E_p^*$, V
5.0×10^{-4}	−0.750	1.30	−0.920	−0.64	0.49	0.170
2.5×10^{-4}	−0.725	0.58	−0.905	−0.25	0.42	0.180
1.0×10^{-4}	−0.695	0.22	−0.900	−0.091	0.42	0.205
5.0×10^{-5}	−0.680	0.096	−0.895	−0.040	0.41	0.215
2.5×10^{-5}	−0.650	0.041	−0.890	−0.017	0.42	0.240
1.0×10^{-5}	−0.620	0.015	−0.890	−0.0059	0.41	0.270

[a] Dropping-mercury electrode, t = 0.5 s, pulse amplitude −50 mV. [b] Peak corresponding to negative differential current i_p^*. [c] V vs. Ag/AgCl (satd LiCl; CH_2Cl_2). $E_{1/2}[(C_5H_5)_2Fe^+/(C_5H_5)_2Fe]$ = +0.480 V vs. Ag/AgCl (satd LiCl; CH_2Cl_2).

Table III. Polarographic Data for the Reduction Responses of Mixed-Ligand Complexes $Hg(RR'dtc)_2(PX_3)_n$ (5×10^{-4} M) in Dichloromethane (0.1 M Bu_4NClO_4) at 20 °C

R	R′	X	$[PX_3]$, M	dc polarography[a] $E_{1/2}$, V[d]	differential pulse polarography[a,b] E_p, V[d]	E_p,[c] V[d]	comments
c-Hx	c-Hx	c-Hx	0	−0.745	−0.740		current suppression gradual over the potential range
			1×10^{-3}	−0.805	−0.800	−0.910	−0.85 to −1.6 V, no "plateau" region of limiting current
$-(CH_2)_4-$		c-Hx	0	−0.635	−0.640		limiting current region spanning ≈0.2 V followed by
			1×10^{-3}	−0.735	−0.730	−1.085	sharp current suppression
n-Bu	*n*-Bu	*n*-Bu	0	−0.660	−0.665		limiting current region spanning ≈0.15 V, then gradual
			1×10^{-3}	−0.730	−0.730	−0.965	decrease in current
n-Bu	*n*-Bu	Ph	0	−0.660	−0.665		no current suppression or negative differential
			1×10^{-3}	−0.660	−0.660		current observed

[a] Dropping-mercury electrode, t = 0.5 s. [b] Pulse amplitude −50 mV. [c] Peak corresponding to a negative differential current. [d] V vs. Ag/AgCl (satd LiCl; CH_2Cl_2). $E_{1/2}[(C_5H_5)_2Fe^+/(C_5H_5)_2Fe]$ = +0.480 V vs. Ag/AgCl (satd LiCl; CH_2Cl_2).

ligand is an extremely important factor since P-c-Hx_3 and PBu_3 are known to be significantly more basic than PPh_3.[25]

In discussing the electrochemical phenomena arising from mercury dithiocarbamate–phosphine complexes, we note that other workers have reported apparently similar behavior. However, in each case explanations given in their work have proved not applicable to the present system. Nagaosa and Tanaka[19] have shown that a dc polarographic minimum (current suppression) occurs in the reduction response for the tetraiodocadmate ion ($[CdI_4]^{2-}$) in acetonitrile. It was found that the minimum could be reduced in magnitude or removed totally by variation of the cation in the supporting electrolyte, particularly by addition of species possessing large or highly charged cations. It was thus concluded that the minimum resulted from electrostatic repulsion between the cadmate anion and the negatively charged electrode surface and that the cations present at the electrode surface alleviated the suppression to varying extents. As mentioned earlier, large changes in both the cation and anion of the supporting electrolyte produced no significant changes in the behavior of the mercury dithiocarbamate–phosphine system. The fact that significant concentrations of charged species are unlikely to be present in the solutions is consistent with the observed results. The work of Pospíšil and DeLevie[23] on the reduction of aqueous indium(III) in the presence of thiocyanate is similar to that of Nagaosa and Tanaka. For indium, however, the reduction is catalyzed by adsorbed thiocyanate and at potentials in the limiting-current region a dc polarographic minimum results from increased repulsion between the electrode and the adsorbed catalyst.

Another example of dc polarographic minima has been reported by Müller et al.[24] in their study of aqueous copper(II) reduction in the presence of tertiary phosphine oxides. These authors have shown that the DME is fully covered by a phosphine oxide film and that a correlation exists between film pressure and the rate of the electrode reaction. In contrast, with the mercury dithiocarbamate–phosphine system, however, it was found that the potential range over which current suppression occurred steadily increased as additions of phosphine oxides were made. Thus, small additions produced a minimum only in the limiting-current region while further additions extended the current suppression well into the rising portion of the polarographic wave. Another difference with the present case lies in the fact that the current for copper(II) reduction always returns to the diffusion-controlled value at potentials prior to the solvent reduction. Such results seen by Müller et al. were never observed in the case of the mercury dithiocarbamate–phosphine complexes.

Recently, curve crossing in cyclic voltammetry has been considered by Fox and Akaba[26] for a novel oxidation process. Previous examples of curve crossing have arisen from catalytic reduction processes.[27-30] Feldberg et al.[31] have shown that the reaction scheme

$$\begin{aligned} A + e^- &\rightleftarrows B \quad (E) \\ B &\rightarrow C \quad (C) \\ C + e^- &\rightleftarrows D \quad (E) \\ D + A &\rightleftarrows B + C \end{aligned} \qquad (9)$$

should lead to curve crossing in cyclic voltammetry. However, to the best of our knowledge this kind of phenomenon has been neither observed nor predicted for labile mixed-ligand complexes where electrochemical processes for the contributing species do not exhibit such behavior.

All of our data indicate that mixed-ligand-complex formation is responsible for the unusual electrochemical phenomena. The experiments with varying concentration ratios of the two ligands indicate that the complexes $Hg(RR'dtc)_2(PX_3)_n$ (n = 1, 2) are dominant.

NMR spectroscopy provides a convenient method for examining the nature of possible mixed-ligand complexes in this system.[12] However, insufficient data are available in the previous report, and some additional studies were undertaken to ascertain the nature of the relevant mixed-ligand complexes.

For mixtures of a mercury dithiocarbamate and either PBu_3 or P-c-Hx_3 it was shown that rapid exchange occurs at room temperature according to reaction 3. Phosphorus-31 NMR spectra

(25) Goldwhite, H. *Introduction to Phosphorus Chemistry*; Cambridge University Press: Cambridge, 1981; p 42.

(26) Fox, M. A.; Akaba, R. *J. Am. Chem. Soc.* **1983**, *105*, 3460.
(27) Savéant, J. M. *Acc. Chem. Res.* **1980**, *13*, 323.
(28) Amatore, C.; Pinson, J.; Savéant, M. M.; Thiebautt, A. *J. Electroanal. Chem. Interfacial Electrochem.* **1979**, *107*, 59.
(29) Amatore, C.; Pinson, J.; Savéant, J. M.; Thiebautt, A. *J. Electroanal. Chem. Interfacial Electrochem.* **1979**, *107*, 75.
(30) Bard, A. J. *J. Electrochem. Soc.* **1977**, *124*, 189.
(31) Feldberg, S. W. *J. Phys. Chem.* **1971**, *75*, 2377 and references cited therein.

Table IV. ^{31}P and ^{199}Hg NMR Data[a] for the Mixed-Ligand Complexes $Hg(RR'dtc)_2(PX_3)_n$ in Dichloromethane Solution

Hg-(RR'dtc)$_2$ R	R'	X	n	$\delta(^{31}P)$[b]	$\delta(^{199}Hg)$[c]	$J_{Hg,P}$, Hz	T, °C
Et	Et	c-Hx	1	45.7	499	5465	−90
			2	50.6	892	3900	−90
n-Pr	*n*-Pr	c-Hx	1	44.9	581	5425	−90
			2	49.7	894	3885	−90
n-Bu	*n*-Bu	c-Hx	1	45.6	582	5420	−90
			2	50.6	897	3885	−90
c-Hx	c-Hx	c-Hx	1	43.7	633	5240	−110
			2	48.6	947	3860	−110
Et	Et	*n*-Bu	1	18.9	614	5635	−90
			2	4.5	908	4870	−90
n-Pr	*n*-Pr	*n*-Bu	1	18.7	618	5635	−90
			2	13.7	904	4890	−90
n-Bu	*n*-Bu	*n*-Bu	1	17.4	615	5570	−90
			2	12.6	900	4925	−90
c-Hx	c-Hx	*n*-Bu	1	17.5	665	5450	−110
			2	10.8	903	4965	−110
heterocyclic derivatives							
pip		c-Hx	1	45.7	584	5500	−90
			2	50.8	895	3870	−90
pyrr		c-Hx	1	50.0	*d*	*d*	−100
			2	*e*	*e*		
pip		*n*-Bu	1	19.2	622	5890	−90
			2	14.9	899	4915	−90
pyrr		*n*-Bu	1	23.0	822	5210	−100

[a] Data for some $Hg(RR'dtc)(P\text{-}n\text{-}Bu_3)_n$ and $Hg(RR'dtc)_2(P\text{-}c\text{-}Hx_3)_n$ complexes have been reported in ref 12. [b] Reference: 85% phosphoric acid in water. [c] Reference: 1 M phenylmercury acetate in Me_2SO. [d] Exchange still rapid at −100 °C. [e] Not recorded.

at room temperature therefore show broad average signals for the species present. However, at temperatures around −90 °C the exchange is effectively slowed and signals for all the species present may be observed. Data for mixtures of mercury dithiocarbamates and phosphine are given in Table IV. Figure 12 shows the mercury-199 and phosphorus-31 NMR spectra for a dichloromethane solution containing the stoichiometric proportions $Hg(n\text{-}Bu_2dtc)_2$:P-c-Hx_3 = 1:2, which reveal that at this temperature the equilibrium constant K for the reaction

$$Hg(n\text{-}Bu_2dtc)_2PX_3 + PX_3 \overset{K}{\rightleftharpoons} Hg(n\text{-}Bu_2dtc)_2(PX_3)_2 \qquad (10)$$

$$K = \frac{[Hg(n\text{-}Bu_2dtc)_2(PX_3)_2]}{[Hg(n\text{-}Bu_2dtc)_2PX_3][PX_3]}$$

is such that all three species coexist in significant concentrations. NMR spectra (phosphorus-31) were recorded for a series of mercury dithiocarbamate–tricyclohexylphosphine mixtures at five temperatures. In each case values of K were calculated by using the signal area for the concentration of each species. This data allowed the determination of ΔH for reaction 10 using the Clausius–Clapeyron equation, and the results are shown in Table V. The extrapolation of this data to room temperature enables equilibrium constants to be calculated for conditions under which most of the electrochemical data were obtained. Different ionic strengths were assumed not to be significant. The resulting equilibrium data show that $Hg(RR'dtc)_2P\text{-}c\text{-}Hx_3$ is the major

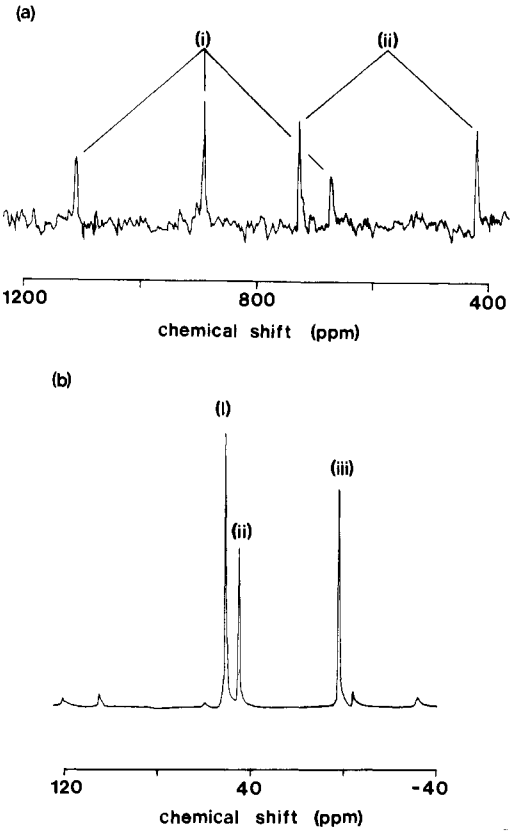

Figure 12. NMR spectra for a solution in dichloromethane containing $Hg(n\text{-}Bu_2dtc)_2$ and P-c-Hx_3 at −90 °C: (a) mercury-199 NMR spectrum showing signals for (i) $Hg(n\text{-}Bu_2dtc)_2(P\text{-}c\text{-}Hx_3)_2$ and (ii) $Hg(n\text{-}Bu_2dtc)_2P\text{-}c\text{-}Hx_3$; (b) phosphorus-31 NMR spectrum showing signals for (i) $Hg(n\text{-}Bu_2dtc)_2(P\text{-}c\text{-}Hx_3)_2$ (ii) $Hg(n\text{-}Bu_2dtc)_2P\text{-}c\text{-}Hx_3$, and (iii) P-c-$Hx_3$.

species in the bulk solution (Table V) under the conditions of electrochemistry (T = 20 °C).

The new polarographic wave ($E_{1/2}$ = −0.73 V) is therefore assigned to the overall process

$$Hg(RR'dtc)_2P\text{-}c\text{-}Hx_3 + 2e^- \rightleftarrows Hg + 2RR'dtc^- + P\text{-}c\text{-}Hx_3 \qquad (11)$$

The complex $Hg(RR'dtc)_2P\text{-}c\text{-}Hx_3$ could contain both mono- and bidentate dithiocarbamate ligands, and the possibility of polymer formation was investigated via molecular weight measurements on a range of dichloromethane solutions containing $Hg(n\text{-}Bu_2dtc)_2$ and P-c-Hx_3. All molecular weight data were consistent with the presence of only monomeric species in solution.

The origin of the current reversal (cyclic voltammetry), negative differential current (differential pulse polarography), and current suppression (dc polarography) appears to be associated with a stoichiometry for Hg:RR'dtc:P-c-Hx_3 of 1:2:2 since the effects continue to increase after the 1:2:1 stoichiometry has been reached. At the potentials where these phenomena occur, each of the complexes $[Hg(P\text{-}c\text{-}Hx_3)_2]^{2+}$, $Hg(RR'dtc)_2$, and $Hg(RR'dtc)_2P\text{-}c\text{-}Hx_3$ has been reduced to elemental mercury and the free ligands. All of these processes require the complete disproportionation of

Table V. Equilibrium Data for the Following Reaction in Dichloromethane:

$$Hg(RR'dtc)_2P^a + P \overset{K}{\rightleftharpoons} Hg(RR'dtc)_2P_2$$

$Hg(RR'dtc)_2$ R	R'	K (=$[Hg(RR'dtc)_2P_2]/[Hg(RR'dtc)_2P][P]$), M^{-1} −60 °C	−70 °C	−80 °C	−90 °C	−100 °C	ΔH, kJ mol^{-1}	$K_{20°C}$, M^{-1}
Et	Et	0.269	0.621	1.47	3.79	11.2	−28.5	3.36×10^{-3}
n-Pr	*n*-Pr	1.48	3.28	7.55	20.3	60.1	−28.4	1.80×10^{-2}
n-Bu	*n*-Bu	0.445	1.01	2.39	6.31	19.0	−29.1	4.95×10^{-3}
c-Hx	c-Hx		0.642	0.831	1.09	1.55	−8.70	0.124
$-(CH_2)_5-$		1.74	3.01	5.35	10.4	21.8	−39.2	2.33×10^{-3}

[a] P denotes tricyclohexylphosphine, P-c-Hx_3.

mercury(I) intermediates (see eq 6 and 7). A tentative explanation for the phenomena associated with current depression (dc polarography) is that a mixed mercury(I) complex of the type $Hg(RR'dtc)P\text{-}c\text{-}Hx_3$ (structural information and stoichiometry unknown) is more stable toward disproportionation than are the nonmixed mercury(I) complexes. That is, at potentials more negative than any of the other reduction processes the reactions

$$Hg(RR'dtc)_2 + Hg + 2P\text{-}c\text{-}Hx_3 \rightleftarrows 2Hg(RR'dtc)P\text{-}c\text{-}Hx_3 \quad (12)$$

$$[Hg(P\text{-}c\text{-}Hx_3)_2]^{2+} + Hg + 2RR'dtc^- \rightleftarrows 2Hg(RR'dtc)P\text{-}c\text{-}Hx_3 \quad (13)$$

$$Hg(RR'dtc)_2P\text{-}c\text{-}Hx_3 + Hg + P\text{-}c\text{-}Hx_3 \rightleftarrows 2Hg(RR'dtc)P\text{-}c\text{-}Hx_3 \quad (14)$$

all lie to the right and involve no net electron transfer. The mechanism of formation of $Hg(RR'dtc)P\text{-}c\text{-}Hx_3$ could also be envisaged as occurring via the redox process

$$Hg + RR'dtc^- + P\text{-}c\text{-}Hx_3 \rightleftarrows Hg(RR'dtc)P\text{-}c\text{-}Hx_3 + e^- \quad (15)$$

to give an $\bar{E}\bar{E}$ reaction (coupled with chemical steps) resulting in no net electron transfer. An alternative view of this reaction mechanism is that the process

$$Hg(RR'dtc)_2(P\text{-}c\text{-}Hx_3)_2 + 2e^- \rightleftarrows Hg + 2RR'dtc^- + 2P\text{-}c\text{-}Hx_3 \quad (16)$$

is forbidden on thermodynamic grounds because of the preference for the reactants and products of reaction 16 to undergo the reaction

$$Hg(RR'dtc)_2(P\text{-}c\text{-}Hx_3)_2 + 3Hg + 2RR'dtc^- + 2P\text{-}c\text{-}Hx_3 \rightleftarrows 4Hg(RR'dtc)P\text{-}c\text{-}Hx_3 + 2e^- \quad (17)$$

where additional mercury is provided by the electrode. While we admit that the details of this novel mechanism cannot be assigned with complete confidence, mixed-ligand-complex formation does seem to be a dominant factor in causing the observed responses. Theoretical studies by Feldberg and Jeftic have addressed nuances of the $\bar{E}C\bar{E}$ mechanism[32] where the electron-transfer steps are first-order reversible processes. Unfortunately, the present case includes nonunity-order electron-transfer steps and we were unable to undertake the digital simulation theory required to simulate this class of electron-transfer coupled with a cross-redox reaction as would be required in the present instance.

Not surprisingly, the electrochemistry of mixtures of $Hg(RR'dtc)_2$ and $[Hg(P\text{-}c\text{-}Hx_3)_2]^{2+}$ is quite complex. Importantly, the previously mentioned phenomena of current reversal, negative differential currents, and current suppression are all observed. The oxidation process[10] for $Hg(RR'dtc)_2$ are modified, and two new well-defined reduction processes ($E_{1/2} = -0.12$ V; $E_{1/2} = -0.60$ V) are observed (see Figure 13). The equilibrium

$$Hg(RR'dtc)_2 + [Hg(P\text{-}c\text{-}Hx_3)_2]^{2+} \rightleftarrows 2[Hg(RR'dtc)P\text{-}c\text{-}Hx_3]^+ \quad (18)$$

is presumed to be important in that on reduction of $[Hg(RR'dtc)P\text{-}c\text{-}Hx_3]^+$ and/or $Hg(P\text{-}c\text{-}Hx_3)_2]^{2+}$ to generate the ligands and elemental mercury the reaction between $Hg(RR'dtc)_2$ and $P\text{-}c\text{-}Hx_3$ will proceed to give $Hg(RR'dtc)P\text{-}c\text{-}Hx_3$ and the unusual electrochemical phenomena. Unfortunately, no direct measurement of the stabilities of the different Hg(I) intermediates can be made. However, the species $Hg(RR'dtc)P\text{-}c\text{-}Hx_3$ may have a geometry that along with its charge neutrality gives enhanced stability relative to other Hg(I) complexes.

(32) Feldberg, S. W.; Jeftic, L. *J. Phys. Chem.* **1972**, *76*, 2439.

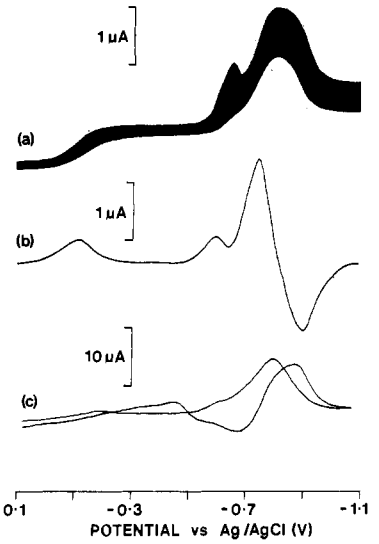

Figure 13. Electrochemical reduction responses for a solution containing $Hg(n\text{-}Bu_2dtc)_2$ (5×10^{-4} M) and $[Hg(P\text{-}c\text{-}Hx_3)_2](ClO_4)_2$ (5×10^{-4} M): (a) dc polarogram (drop time 0.5 s); (b) differential pulse polarogram (drop time 0.5 s, pulse amplitude −50 mV); (c) cyclic voltammogram (DME, scan rate 500 mV s^{-1}).

Appendix of Symbols and Abbreviations

E	potential
i	current
$E_{1/2}$	half-wave potential—defined by $i = (1/2)i_d$
i_d	limiting diffusion-controlled current
i_l	limiting current
E_p	peak potential
i_p	peak current
dc	direct current
E_p^{red}	peak potential for reduction in cyclic voltammetry
E_p^{ox}	peak potential for oxidation in cyclic voltammetry
k	rate constant
$\bar{E}\bar{E}$	electrochemical reduction followed by electrochemical oxidation
DME	dropping-mercury electrode
HMDE	hanging-mercury-drop electrode
NMR	nuclear magnetic resonance
δ	NMR chemical shift
J	NMR coupling constant (Hz)
dtc	dithiocarbamate
c-Hx	cyclohexyl
Bz	benzyl
pyrrdtc	pyrrolidine-*N*-carbodithioate
pipdtc	piperidine-*N*-carbodithioate

Registry No. $Hg(n\text{-}Bu_2dtc)_2(P(c\text{-}Hx)_3)_2$, 101011-34-1; $Hg(n\text{-}Bu_2dtc)_2(P(c\text{-}Hx)_3)$, 79573-00-5; $Hg(Et_2dtc)_2(P(c\text{-}Hx)_3)$, 101011-35-2; $Hg(Et_2dtc)_2(P(c\text{-}Hx)_3)_2$, 101011-36-3; $Hg(Pr_2dtc)_2(P(c\text{-}Hx)_3)$, 101011-37-4; $Hg(Pr_2dtc)_2(P(c\text{-}Hx)_3)_2$, 101011-38-5; $Hg(c\text{-}Hx_2dtc)_2(P(c\text{-}Hx)_3)$, 101011-39-6; $Hg(c\text{-}Hx_2dtc)_2(P(c\text{-}Hx)_3)_2$, 101011-40-9; $Hg(Et_2dtc)_2(PBu_3)$, 101011-41-0; $Hg(Et_2dtc)_2(PBu_3)_2$, 101011-42-1; $Hg(Pr_2dtc)_2(PBu_3)$, 101011-43-2; $Hg(Pr_2dtc)_2(PBu_3)_2$, 101011-44-3; $Hg(Bu_2dtc)_2(PBu_3)$, 79572-87-5; $Hg(Bu_2dtc)_2(PBu_3)_2$, 79572-88-6; $Hg(c\text{-}Hx_2dtc)_2(PBu_3)$, 101011-45-4; $Hg(c\text{-}Hx_2dtc)_2(PBu_3)_2$, 101011-46-5; $Hg((CH_2)_5dtc)_2(P(c\text{-}Hx)_3)$, 79573-01-6; $Hg((CH_2)_5dtc)_2(P(c\text{-}Hx)_3)_2$, 101011-47-6; $Hg((CH_2)_4dtc)_2(P(c\text{-}Hx)_3)$, 101011-48-7; $Hg((CH_2)_4dtc)_2(P(c\text{-}Hx)_3)_2$, 101011-49-8; $Hg((CH_2)_5dtc)_2(PBu_3)$, 101031-38-3; $Hg((CH_2)_5dtc)_2(PBu_3)_2$, 101011-50-1; $Hg((CH_2)_4dtc)_2(PBu_3)$, 101011-51-2; $Hg(n\text{-}Bu_2dtc)_2$, 21439-58-7; $Bu_4N(n\text{-}Bu_2dtc)$, 71195-46-5; P-c-Hx_3, 2622-14-2; Bu_4NClO_4, 1923-70-2; Et_4NClO_4, 2567-83-1; c-Hx_4ClO_4, 101011-52-3; Bu_4NPF_6, 3109-63-5; Bu_4NBPh_4, 15522-59-5; ^{199}Hg, 14191-87-8; $[Hg(P\text{-}c\text{-}Hx_3)_2](ClO_4)_2$, 66119-63-9.